Large Scale Structures in Rayleigh-Bénard Convection at High Rayleigh Numbers

T. Hartlep and A. Tilgner
Institute of Geophysics, University of Göttingen, Herzberger Landstraße 180, 37075 Göttingen, Germany

F. H. Busse
Institute of Physics, University of Bayreuth, 95440 Bayreuth, Germany
(Received 21 February 2003; published 4 August 2003)

Direct numerical simulations of Rayleigh-Bénard convection in a plane layer with periodic boundary conditions at Rayleigh numbers up to 10^7 show that flow structures can be objectively classified as large or small scale structures because of a gap in spatial spectra. The typical size of the large scale structures does not always vary monotonically as a function of the Rayleigh number but broadly increases with increasing Rayleigh number. A mean flow (whose average over horizontal planes differs from zero) is also excited but is weak in comparison with the large scale structures. The large scale circulation observed in experiments should therefore be a manifestation of the large scale structures identified here.

DOI: 10.1103/PhysRevLett.91.064501 PACS numbers: 47.27.Te, 44.25.+f

The investigation of convection at high Rayleigh number Ra, both experimental and numerical, has for practical reasons mostly been limited to convection in boxes of aspect ratio near unity [1–4]. On the other hand, applications frequently invoked as a motivation for these studies involve geometries of very large aspect ratios as, for example, atmospheric convection. The presence of lateral walls should, however, be decisive for the large scale circulation.

It has been noted in experiments with containers of aspect ratio around one that a coherent flow encompassing the entire box persists up to the highest Ra reached [4–6]. The fluid flows horizontally in one direction along the bottom plate and in the opposite direction near the top plate with connecting flows along the side walls. Even in containers of larger aspect ratio, some authors have observed a single circulation running through the container limited in its size only by lateral walls [7]. The presence of this "wind" has played a major role in theories attempting to explain the Rayleigh number dependence of the Nusselt number [8,9]. Less effort has been made to explain where the large scale circulation comes from in the first place.

According to one point of view, the rolls which develop at low Ra near the onset of convection continually increase their size as Ra is increased and continue to exist in an averaged sense at even the highest Ra reached in experiments. This view is supported by measurements in air [10]. Another hypothesis holds that the large scale circulation is a genuine high Rayleigh number effect in which plumes erupting from the boundary layers interact with the mean shear which tilts the plumes. The tilted plumes in turn generate a Reynolds stress which maintains the shear against dissipation [7].

In order to shed light on these issues, we investigate by direct numerical simulation thermal convection at Ra up to 10^7 in plane layers. Periodic boundary conditions are used in the horizontal directions. The ratio of the periodicity length and the vertical extent of the layer is typically 10, in some runs up to 20.

Consider an infinitely extended plane layer of height d filled with fluid of viscosity ν, thermal diffusivity κ, density ρ, and thermal expansion coefficient α. A Cartesian coordinate system is chosen such that the gravitational acceleration g acts perpendicular to the boundaries of the layer in the negative z direction and that the bottom boundary is located at $z = 0$. The temperature at the bottom exceeds the temperature at the top by ΔT. The boundary conditions for the velocity field are no slip at both boundaries. Periodic boundary conditions are imposed in the x and y directions with periodicity lengths l_x and l_y. The aspect ratio A is defined as $A = l_x/d = l_y/d$. Using d, d^2/κ, ΔT, and $\rho\kappa^2/d^2$ as units of length, time, temperature, and pressure, respectively, one obtains nondimensional equations for the velocity $\boldsymbol{v}(\boldsymbol{r}, t)$ and the temperature $T(\boldsymbol{r}, t)$ which involve in the Boussinesq approximation just two additional control parameters: the Rayleigh number $\mathrm{Ra} = g\alpha d^3\Delta T/(\kappa\nu)$ and the Prandtl number $\mathrm{Pr} = \nu/\kappa$. When the fluid is at rest, the (dimensionless) temperature depends only on z and varies as $T(z = 0) - z$. In the general case, it is convenient to specify the temperature through the deviation Θ from the static profile: $T(\boldsymbol{r}, t) = \Theta(\boldsymbol{r}, t) + T(z = 0) - z$. The equations of motion for $\boldsymbol{v}(\boldsymbol{r}, t)$ and $\Theta(\boldsymbol{r}, t)$ are

$$\partial_t \boldsymbol{v} + (\boldsymbol{v}\cdot\nabla)\boldsymbol{v} = -\nabla p + \mathrm{Pr}\,\nabla^2\boldsymbol{v} + \mathrm{Ra}\,\mathrm{Pr}\,\Theta\hat{\boldsymbol{z}}, \quad (1)$$

$$\nabla\cdot\boldsymbol{v} = 0, \quad (2)$$

$$\partial_t\Theta + \boldsymbol{v}\cdot\nabla\Theta - \boldsymbol{v}\cdot\hat{\boldsymbol{z}} = \nabla^2\Theta, \quad (3)$$

$$\Theta(z = 0) = \Theta(z = 1) = \boldsymbol{v}(z = 0) = \boldsymbol{v}(z = 1) = 0. \quad (4)$$

$\hat{\boldsymbol{z}}$ is the unit vector in the z direction and p is the pressure. The velocity field can be uniquely represented by a

poloidal scalar $\phi(\boldsymbol{r}, t)$, a toroidal scalar $\psi(\boldsymbol{r}, t)$, and a mean flow $\boldsymbol{U}(z, t)$:

$$\boldsymbol{v} = \nabla \times \nabla \times \phi \hat{\boldsymbol{z}} + \nabla \times \psi \hat{\boldsymbol{z}} + \boldsymbol{U}. \quad (5)$$

It follows directly from the boundary conditions and the definition of $\boldsymbol{U}$ that the z component of $\boldsymbol{U}$ must be zero. $\boldsymbol{U}$ is thus a toroidal flow. However, the corresponding toroidal scalar varies linearly in x and y and is unbounded. If ψ is required to stay finite and has to obey periodic boundary conditions, it is necessary to include $\boldsymbol{U}$ in the decomposition of $\boldsymbol{v}$ [11].

$\boldsymbol{U}$ describes a shearing motion extending horizontally to infinity. The word "mean flow" is reserved for such an infinitely extended motion in the theoretical literature on large aspect ratio convection [11,12]. A mean flow $\boldsymbol{U}$ cannot exist in an experiment because of side walls. It is nonetheless important to decide by means of numerical simulation whether a mean flow of significant amplitude exists in an infinite layer. If the dynamics of convection are such that they excite a mean flow in an infinite layer, we expect to find a large scale circulation encompassing the whole experimental cell in cells of any aspect ratio. Suppose on the other hand that $\boldsymbol{U}$ is negligible even in an infinite layer and that the flow at large scales is approximately described as parallel rolls. In an experiment of sufficiently large aspect ratio, we will then find several of these rolls instead of a single circulation filling the whole cell.

Equations of motion for ϕ, ψ, and $\boldsymbol{U}$ are obtained from the z component of the curl of the curl of (1), the z component of the curl of (1), and the average over horizontal planes of (1), respectively. These equations are solved numerically. A spectral method [13,14] is used which discretizes space with Chebychev polynomials in the z direction and with Fourier modes in the x and y directions. Dealiasing with the 2/3 rule was implemented. The time marching procedure is a second order Adams-Bashforth scheme for the advection and buoyancy terms coupled to a Crank-Nicolson scheme for the diffusive terms. An adaptive time step is used to speed up the transients. All computations have been started from random noise as initial conditions and have been run for several tens of convective time scales $\tau = (2E_{\mathrm{kin}})^{-1}$, with $E_{\mathrm{kin}} = A^{-2} \int_0^A \int_0^A \int_0^1 dx\, dy\, dz\, \boldsymbol{v}^2/2$. Spatial resolution was up to 65 Chebychev polynomials and 512^2 grid points in horizontal planes.

Spectral analysis is the most straightforward tool to classify convective structures according to their length scale. One can compute spectra of various quantities which all lead to the same conclusions. We present the spectral distribution of the advective heat transport $H = A^2 \langle v_z \Theta \rangle$ through a horizontal plane. $\langle \cdots \rangle$ denotes the average over the plane. Expressed in terms of the discrete Fourier transforms $\mathcal{F}_{v_z}$ (vertical velocity) and $\mathcal{F}_\Theta$ (temperature), the heat transport H reads

$$H = \sum_i \Delta\lambda \left\{ \sum_{\boldsymbol{k} \text{ with } \lambda_i \le (2\pi)/|\boldsymbol{k}| < \lambda_{i+1}} \frac{\mathrm{Re}\{\mathcal{F}^*_{v_z}(\boldsymbol{k}) \mathcal{F}_\Theta(\boldsymbol{k})\}}{\Delta\lambda N_x N_y} \right\}. \quad (6)$$

N_x and N_y are the number of Fourier modes in x and y directions, respectively, $\boldsymbol{k} = (kx, ky)$ is a wave vector in the horizontal plane, and $\Delta\lambda = \lambda_{i+1} - \lambda_i$. The expression in the curly braces represents the spectral density $\widehat{v_z\Theta}$ of the advective heat transport. $\widehat{v_z\Theta}$ is assumed constant in the intervals $[\lambda_i, \lambda_i + \Delta\lambda]$ and is shown in Fig. 1 for $\Delta\lambda = 0.1$.

All spectra show a gap which allows us to classify wavelengths as "large" or "small" scales. The spectral content of the small scales increases with increasing Ra and in planes closer to the boundaries. The maximum of $\widehat{v_z\Theta}_i$ in the range of the small scales shifts towards smaller λ with increasing Ra. The wavelength of the maximum at large λ, $\lambda_{\max}$, most conveniently characterizes the large scales. $\lambda_{\max}$ can assume only a few different discrete values due to the periodic boundary conditions. For instance, the largest possible values for λ/A are 1, $1/\sqrt{2}$, 1/2, $1/\sqrt{5}$, $1/\sqrt{8}$, ... without any values in between. $\lambda_{\max}$ therefore varies in steps as a function of Ra or Pr. A smoother variation is obtained if one considers an average wavelength $\bar{\lambda} = \sum' \lambda \widehat{v_z\Theta} / \sum' \widehat{v_z\Theta}$, where $\sum'$ denotes the sum over all wavelengths between $\lambda_{\max}/\sqrt{2}$ and $\lambda_{\max}\sqrt{2}$. $\lambda_{\max}$ and $\bar{\lambda}$ never differ by more than 10%. Figure 2 shows $\lambda_{\max}$ as a function of Ra in air, i.e., Pr = 0.7. Both the experimental and numerical values increase in steps with increasing Ra because of the limited number of possible values of $\lambda_{\max}$ in any given geometry. The numerical data are on average somewhat smaller than the experimental numbers. One observes at any rate a general increase of $\lambda_{\max}$ with Ra and the $\lambda_{\max}$ at the highest Ra exceeds the aspect ratio of the containers

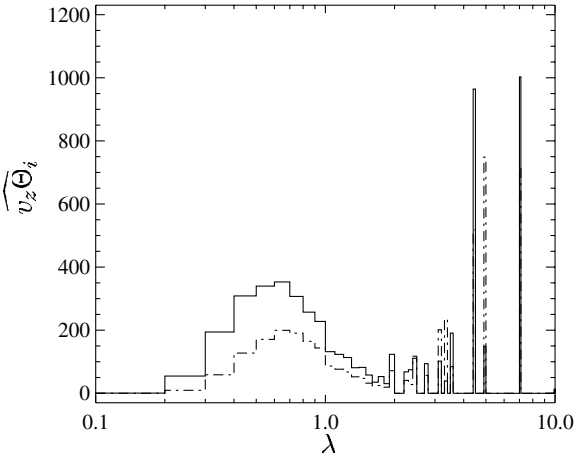

FIG. 1. $\widehat{v_z\Theta}$ as a function of wavelength λ in the midplane ($z = 0.5$) for Pr = 7 and Ra = 10^5 (dashed line) and 2.5×10^5 (continuous line).

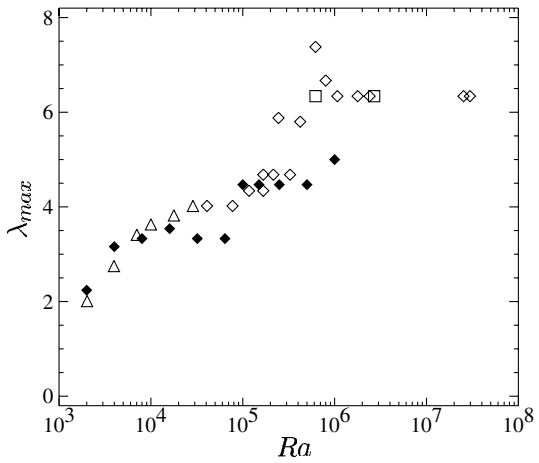

FIG. 2. $\lambda_{\max}$ as a function of Ra for Pr = 0.7. The full symbols are numerical results for $A = 10$; the open symbols are experimental data compiled in Ref. [10] for rectangular containers with various aspect ratios.

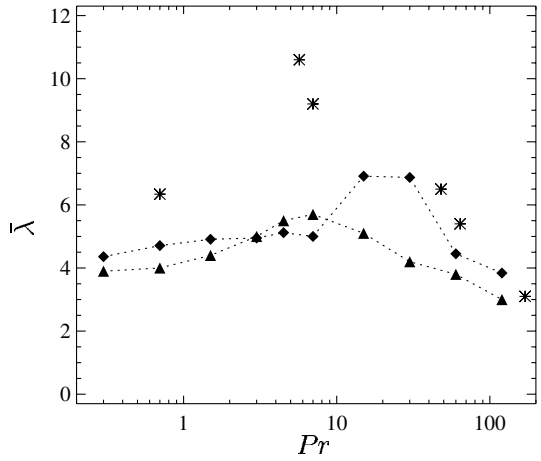

FIG. 3. $\bar{\lambda}$ as a function of Pr for Re = 10^5 (triangles) and 10^6 (diamonds). Stars are experimental data from Refs. [10,15].

customarily used for experiments at large Rayleigh numbers.

$\lambda_{\max}$ coincides with the wavelength of the largest structures identified visually in, for example, contour plots of Θ in the midplane of the layer. Rolls reminiscent of the convection rolls known from the onset of convection remain visible in movies of the flow up to the highest Ra simulated.

In addition to the large scale rolls, a mean flow is also excited in the simulation (i.e., $\boldsymbol{U} \neq 0$), which corresponds to a structure of infinite wavelength. However, the energy contained in this mean flow is less than 0.8% of the total kinetic energy in all investigated cases. The mean flow has an amplitude much smaller than the modes contributing to the structure of size $\lambda_{\max}$. The mean flow is also very time dependent. Its long term average is zero because the mean flow runs in different directions at different times. The temporal average of the magnitude of the mean flow velocity, $|\boldsymbol{U}|$, is comparable with the rms of the fluctuations of $|\boldsymbol{U}|$.

Figure 3 shows $\bar{\lambda}$ as a function of Pr for Ra = 10^5 and 10^6 together with experimental data. It is seen that, for any Ra, $\bar{\lambda}$(Pr) goes through a maximum. This fact is already indicated by the experimental data which are, however, collected at varying Rayleigh numbers and aspect ratios, but the presence of such a maximum is confirmed by the more controlled and systematic numerical simulations. Another piece of information can be gleaned from Ref. [16] which reports simulations of 2D convection at infinite Prandtl number. In this limit, one finds $\bar{\lambda} = 3.3$ at Ra = 10^6. $\bar{\lambda}$ thus asymptotes to a finite value for Pr $\rightarrow \infty$.

In water, Krishnamurti and Howard [7] report a transition of $\bar{\lambda}$ at Ra $\approx 2 \times 10^6$. At low Rayleigh numbers, they observe cellular convection with horizontal length scales comparable with the layer thickness, which is replaced by randomly appearing transient plumes, as the Rayleigh number is increased. At Ra $\approx 2 \times 10^6$, the plumes start to tilt and a large scale flow with length scales comparable to the width of the container (aspect ratio 9.6) is generated. In simulations for Pr = 7 and $A = 10$, there is no sign of such a transition for Rayleigh numbers up to 10^7. The mean flow $\boldsymbol{U}$ exists but it is again too weak and too erratic to account for the experimental observations. These computations have been repeated with small inclinations of the direction of gravity with respect to the normal to the layer. In another series of simulations, the Fourier modes were selected such as to reproduce lateral walls with free slip boundary conditions. None of these ingredients helped in explaining the transition reported in Ref. [7].

The case Pr = 7 is computationally cumbersome because it is near a dividing line between two different forms of convection: Rolls at lower Pr and cellular structures at higher Pr. Both styles of convection may coexist, or the flow may switch from one type of flow to the other in the course of time. Lengthy integrations are thus necessary at Pr = 7. More accurate results can be obtained at both lower (Fig. 2) and larger Pr (Fig. 4). In both cases, one observes a general increase of $\lambda_{\max}$ or $\bar{\lambda}$ with Ra.

In some experiments [15], the aspect ratio was larger than can be routinely simulated numerically. It is therefore important to probe the sensitivity of the results to the aspect ratio. At $A = 10$, Pr = 0.7, and Ra = 10^6, one finds $\lambda_{\max} = 5$ and the rolls lie parallel to either the x or y axis, depending on initial conditions. If $A = 10/\sqrt{2}$ is used, the rolls form an angle of 45° with the coordinate axes thus preserving $\lambda_{\max} = 5$. At least in this particular example, a change of the aspect ratio was insignificant.

In summary, it has been shown in this paper that convective flow contains structures of large but finite

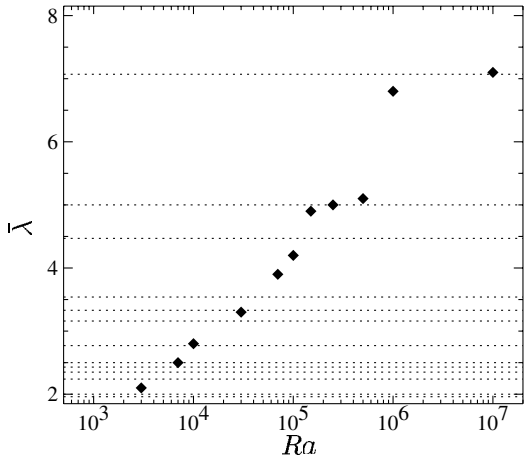

FIG. 4. $\bar{\lambda}$ as a function of Ra for Pr = 30. The dashed horizontal lines indicate the wavelengths of modes satisfying the periodic boundary conditions in a box with $A = 10$.

size in addition to the fluctuations usually associated with turbulence. The two types of structures are separated by a gap in spatial spectra. With increasing Ra, the separation of scales becomes more pronounced because the small scales are increasingly excited at high Ra, whereas the large scales are continuations of the structures already present in laminar flows. In addition, the spectral gap becomes wider with increasing Ra because the large scale structures acquire larger wavelengths, whereas the small scale structures shift towards smaller wavelengths. It cannot be decided from our simulations whether the large scale structures will eventually disappear at yet higher Ra. The simulations have shown, however, that large scale structures exist in the range of Ra normally classified as turbulent and in which even some features of "hard turbulence" are found [14].

The simulations presented here show that the mean flow contains little energy. The large scale circulation detected in experiments is thus better interpreted as a convection roll rather than a mean flow. The large scale structures at high Ra have a large enough wavelength so that a single specimen fills experimental boxes typically in use nowadays. Experiments at larger aspect ratios are necessary in order to learn more about the large scale circulation.

This work was supported by the Deutsche Forschungsgemeinschaft (DFG) and the High Performance Computing Center Stuttgart (HLRS).

[1] R. M. Kerr, Phys. Rev. Lett. **87**, 244502 (2001).
[2] X. Chavanne, F. Chilla, B. Castaing, B. Hébral, B. Chabaud, and J. Chaussy, Phys. Rev. Lett. **79**, 3684 (1997).
[3] X. Xu, K. M. S. Bajaj, and G. Ahlers, Phys. Rev. Lett. **84**, 4357 (2000).
[4] J. J. Niemela, L. Skrbek, K. R. Sreenivasan, and R. J. Donnelly, Nature (London) **404**, 837 (2000).
[5] M. Sano, X. Wu, and A. Libchaber, Phys. Rev. A **40**, 6421 (1989).
[6] G. Zocchi, E. Moses, and A. Libchaber, Physica (Amsterdam) **166A**, 387 (1990).
[7] R. Krishnamurti and L. N. Howard, Proc. Natl. Acad. Sci. U.S.A. **78**, 1981 (1981).
[8] B. Shraiman and S. Siggia, Phys. Rev. A **42**, 3650 (1990).
[9] S. Grossmann and D. Lohse, J. Fluid Mech. **407**, 27 (2000).
[10] D. E. Fitzjarrald, J. Fluid Mech. **73**, 693 (1976).
[11] B. J. Schmitt and W. von Wahl, Diff. Int. Eqs. **5**, 1275 (1992).
[12] E. Bodenschatz, W. Pesch, and G. Ahlers, Annu. Rev. Fluid Mech. **32**, 709 (2000).
[13] R. D. Moser, P. Moin, and A. Leonard, J. Comput. Phys. **54**, 524 (1983).
[14] R. M. Kerr, J. Fluid Mech. **310**, 139 (1996).
[15] F. H. Busse, Acta Mech. [Suppl.] **4**, 11 (1994).
[16] U. Hansen, D. A. Yuen, and S. E. Kroening, Phys. Fluids A **2**, 2157 (1990).